Application of the methylenology principle to substitution reactions. A theoretical study

Hendrik Zipse

Institut für Organische Chemie, TU Berlin, Str. d 17. Juni 135, D-10623 Berlin, Germany

The substitution reaction of chloride with methyl chloride, 2-chloroethyl radical and allyl chloride has been investigated with a number of different *ab initio* theoretical methods. Depending on the theoretical method chosen, the intrinsic barrier for the S_N2' reaction in allyl chloride is 7–11 kcal mol^{-1} higher than the barrier for the S_N2 reaction in methyl chloride. The reaction of chloride with the 2-chloroethyl radical proceeds through formation of an intermediate complex, which can best be characterized as an ethylene fragment flanked by a resonating chloride anion/chloride radical pair. The overall process has been termed '$S_{RN}2^c$', as nucleophilic substitution occurs in this open shell system with overall 'cine' regiochemistry. The intrinsic barrier for the $S_{RN}2^c$ reaction is approximately 10 kcal mol^{-1} lower than that for the S_N2 reaction. The differential barrier heights in these three substitution reactions have been rationalized using the valence bond curve crossing model. The high S_N2' barrier is due to a larger initial excitation energy as compared to the S_N2 reaction and also to a smaller transition state resonance energy. The very low barrier and the formation of an intermediate in the $S_{RN}2^c$ reaction is the consequence of a low lying electronic state, in which homolytic C–Cl bond cleavage has occurred and a C–C double bond is formed. This 'double bond' state descends low enough to cross with the Lewis curves used to describe bond breaking and bond making in nucleophilic substitution reactions in general. Only a small initial excitation is necessary to reach the 'double bond' state from the electronic ground state. This small initial excitation is the origin of the low barrier for the $S_{RN}2^c$ substitution process.

Introduction

The vinylology principle, which states that closed shell reaction systems can be expanded through insertion of vinyl groups while preserving their basic characteristics, has been a fruitful concept in organic chemistry. The comparison of S_N2 and S_N2' reactions involving alkyl and allyl halides serves to illustrate this principle nicely (Scheme 1). It has recently been recognized on the basis of quantum mechanical studies that the vinylology principle can be extended to open shell systems by replacement of the vinyl with a methylene group.[1–3] Appropriately, one would term this new principle the 'methylenology principle'. Scheme 1 includes as an example for the application of this concept the existence of the standard S_N2 mechanism by one methylene group. The most appropriate shortcut designation of this reaction type is '$S_{RN}2^c$', in which the common 'S_N2' abbreviation is extended by 'R' to designate an open shell 'radical' process and by 'c' to describe the overall topology of product formation as 'cine'.[4] One can formally arrive at the $S_{RN}2^c$ reaction not only through addition of a methylene group to the parent system but also by truncation of the allylic double bond in the S_N2' reaction (Scheme 1). We report here an investigation into the three reactions depicted in Scheme 1 with *ab initio* calculations at various levels of sophistication. We will also attempt to rationalize the calculated barrier heights as well as other reaction characteristics through the valence bond curve crossing model (VBCM).[5]

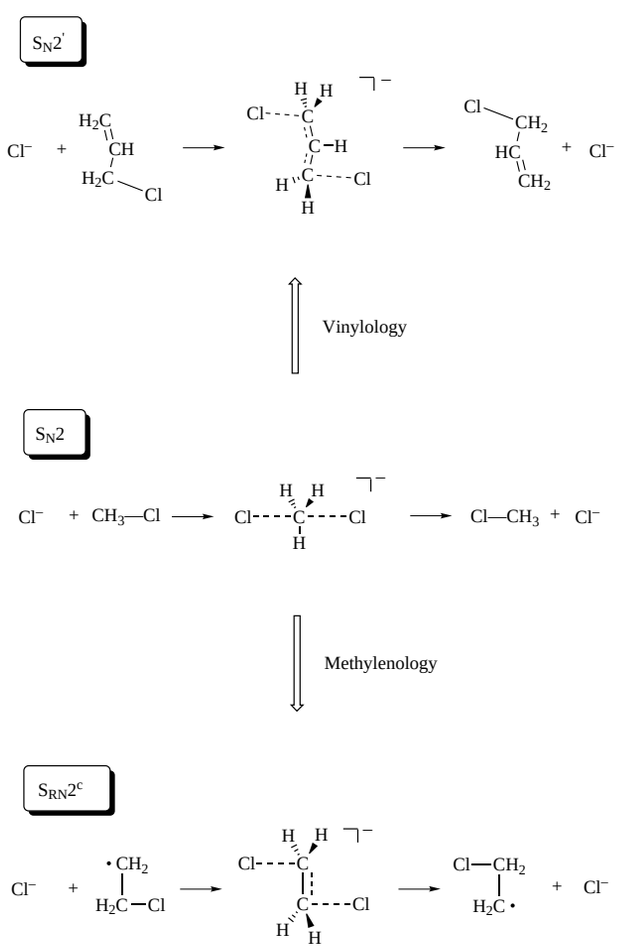

Scheme 1

Theoretical methods

All *ab initio* calculations have been performed with GAUSSIAN94, revision B.[6] Geometry optimizations have been performed at three different levels of theory. (*i*) At the unrestricted Hartree–Fock (UHF) level of theory for open shell systems and at the restricted Hartree–Fock (RHF) level for closed shell systems with the 6-31G(d) basis set. These levels will be referred to as 'HF/6-31G(d)'. (*ii*) At the correlated UMP2(FC)/6-31G(d) level of theory for open shell species and the MP2(FC)/6-31G(d) level for closed shell species. These levels will be referred to as 'MP2/6-31G(d)'. (*iii*) With the Becke-half-and-half LYP hybrid density functional[7] using the 6-31+G(d,p) basis set. This level of theory will be designated 'BHLYP/

Table 1 Energy differences (kcal mol^{-1}) between ground state complexes and transition states in the S_N2, S_N2' and $S_{RN}2^c$ substitution reactions (see text for definitions)

	S_N2		S_N2'		$S_{RN}2^c$		
Level of theory	ΔE_c	ΔE_a	ΔE_c	ΔE_a	ΔE_c	ΔE_a	ΔE_b
UHF/6-31G(d)//UHF/6-31G(d)	−10.3	+13.8	−11.4	+24.6	−10.2	—	+11.3
ZPE (UHF/6-31(d))	+0.3	−0.6	+0.4	−1.0	−0.1	—	+1.0
PMP2/6-31G(d)//MP2/6-31G(d)	−10.9	+15.4	−13.9	+24.2	−11.7	+4.8	+3.9
ZPE (UMP2/6-31G(d))	+0.2	−0.5	+0.4	−0.6	0.0	+1.5	+1.1
PMP2/6-31+G(d,p)//MP2/6-31G(d)	−9.5	+17.2	−12.3	+24.3	−10.3	+5.0	+4.7
PMP2/6-311+G(d,p)//MP2/6-31G(d)	−9.9	+18.0	−12.8	+23.5	−10.8	+4.8	+4.6
PMP2/6-311++G(2d,2p)//MP2/6-31G(d)	−11.0	+13.8	−13.4	+20.8	−11.5	+1.9	+1.3
PMP3/6-311+G(d,p)//MP2/6-31G(d)	−9.9	+18.9	−12.6	+27.4	−10.6	+6.2	+7.1[a]
PMP4/6-311+G(d,p)//MP2/6-31G(d)	−10.0	+16.4	−12.9	+22.8	−10.8	+3.6	+3.4[a]
BHLYP/6-31+G(d,p)//BHLYP/6-31+G(d,p)	−9.8	+12.5[b]	−11.2	+19.6	−9.9	+1.1	+0.3
ZPE (BHLYP/6-31+G(d,p))	+0.1	−0.5	+0.3	−0.8	0.0	+0.8	+0.8

[a] Ref. 1. [b] Ref. 11.

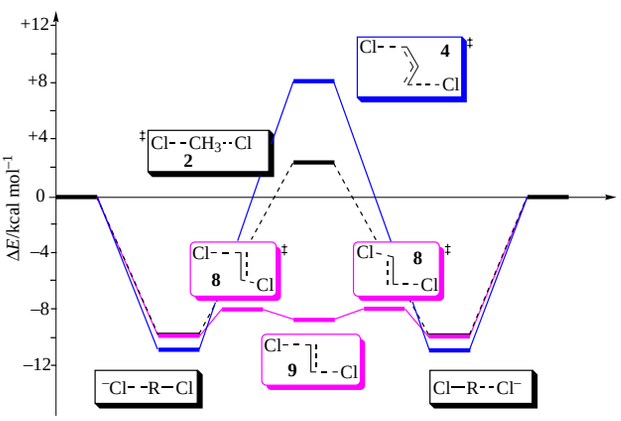

Fig. 1 Schematic representation of the potential energy surface for the S_N2, S_N2' and $S_{RN}2^c$ reactions (drawn to scale at the BHLYP/6-31+G(d,p) + ΔZPE level of theory)

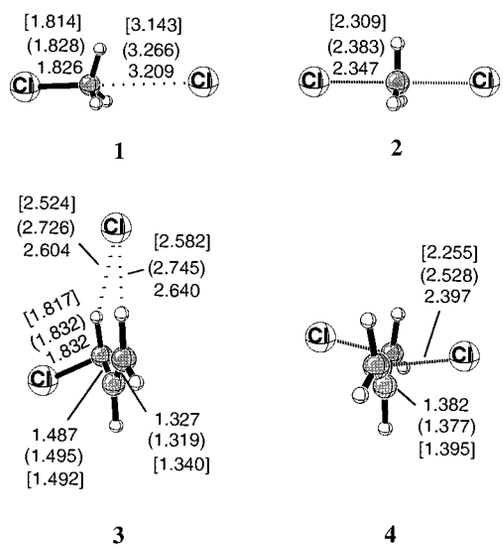

Fig. 2 Structures of ground state complexes and transition states for the S_N2 and S_N2' reactions. Structural data are given at the BHLYP/6-31+G(d,p), HF/6-31G(d) (in brackets) and MP2/6-31G(d) [in square brackets] levels of theory.

6-31+G(d,p)'. In order to study the influence of basis set size as well as the treatment of electron correlation, energies were recalculated using the MP2/6-31G(d) geometries at the MP2 level of theory with the 6-31+G(d,p), 6-311+G(d,p) and 6-311++G(2d,2p) basis sets and at the MP3 and MP4(SDTQ) levels of theory using the 6-311+G(d,p) basis set. Absolute and relative energies obtained with methods based on perturbation theory are obtained after spin projection. Extended Hückel calculations have been performed with YAeHMOP, version 1.1a.[8,†]

Results

The S_N2 reaction between Cl^- and methyl chloride has been previously investigated with various theoretical methods.[9] The potential energy surface for this reaction is shown schematically in Fig. 1 together with those for the S_N2' and $S_{RN}2^c$ reactions. Relative energies are collected in Table 1. The first step in this reaction is the formation of ion–dipole complex **1**, in which the chloride anion coordinates loosely to the methyl hydrogen atoms (Fig. 2). The complexation energy ΔE_c is defined here as the energy difference between the ion–dipole complex and the separate reactants. All theoretical methods used in this study give the same complexation energy within a narrow margin of ±1 kcal mol^{-1}. The best estimates predict a value of ΔE_c = −9.8 kcal mol^{-1} (BHLYP/6-3+G(d,p) + ΔZPE or MP4/6-311+G(d,p)//MP2/6-31G(d) + ΔZPE), which is about 2.5 kcal mol^{-1} more than the experimental value[10] of −8.6 ± 0.2 kcal mol^{-1}. The intrinsic barrier for the S_N2 reaction ΔE_a is defined as the energy difference between transition state **2** and ion–dipole complex **1**. As was already observed for the complexation energy, ΔE_a shows surprisingly little variation with the level of theory. The barrier is only 1.6 kcal mol^{-1} higher at the MP2/6-31G(d) level as compared to the HF/6-31G(d) value. Addition of diffuse basis functions and extension to a valence triple-zeta basis function slightly increases the barrier. The most notable basis set effect occurs upon inclusion of a second polarization function of chlorine which lowers the barrier by almost 4 kcal mol^{-1}.[9d] The PMP3 barrier is slightly higher and the PMP4 barrier is slightly lower than the PMP2 value. Given that barriers computed for the S_N2 reaction at the MP2 and MP4 levels of theory are known to exhibit basis set effects of comparable magnitude,[9d] one can extrapolate the 'MP4/6-311++G(2d,2p)//MP2/6-31G(d) + ΔZPE' barrier to +11.7 kcal mol^{-1}. The barrier height computed at the BHLYP/6-31+G(d,p) + ΔZPE level of theory is slightly higher than this value at +12.0 kcal mol^{-1}. Both values, however, are in near-quantitative agreement with the experimental value of 11.7 ± 0.2 kcal mol^{-1}.[9f,10] These results support the expectation that meaningful estimates can be obtained at these theoretical levels for complexation energies and activation barriers in the S_N2' and $S_{RN}2^c$ reactions. No experimental values appear to be available for the purpose of validation of theoretical predictions in these two cases.

The S_N2' reaction is again initiated through formation of an

† Tables with absolute energies as well as structures for all stationary points are available as supplementary data (SUPPL. NO. 57304, 7 pp.) from the British Library. For details of the Supplementary Publications Scheme, see 'Instructions for Authors', *J. Chem. Soc., Perkin Trans. 2*, 1997, Issue 1.

Table 2 Cumulative charges of alkyl moieties in the S_N2, S_N2' and $S_{RN}2^c$ reactions

	S_N2		S_N2'		$S_{RN}2^c$		
Level of theory	$q(CH_3)$(**1**)	$q(CH_3)$(**2**)	$q(C_3H_5)$(**3**)	$q(C_3H_5)$(**4**)	$q(C_2H_4)$(**6**)	$q(C_2H_4)$(**8**)	$q(C_2H_4)$(**9**)
HF/6-31G(d)//HF/6-31G(d)							
Mulliken	+0.22	+0.49	+0.16	+0.30	+0.19	—	+0.50
CHELPG	+0.33	+0.54	+0.31	+0.36	+0.34	—	+0.55
PMP2/6-31G(d)//MP2/6-31G(d)							
Mulliken	+0.17	+0.32	+0.08	+0.16	+0.13	+0.33	+0.17
CHELPG	+0.29	+0.43	+0.24	+0.29	+0.28	+0.45	+0.31
BHLYP/6-31G(d)//BHLYP/6-31+G(d,p)							
Mulliken	+0.18	+0.36	+0.11	+0.32	+0.16	+0.27	+0.30
CHELPG	+0.29	+0.44	+0.26	+0.40	+0.31	+0.32	+0.37

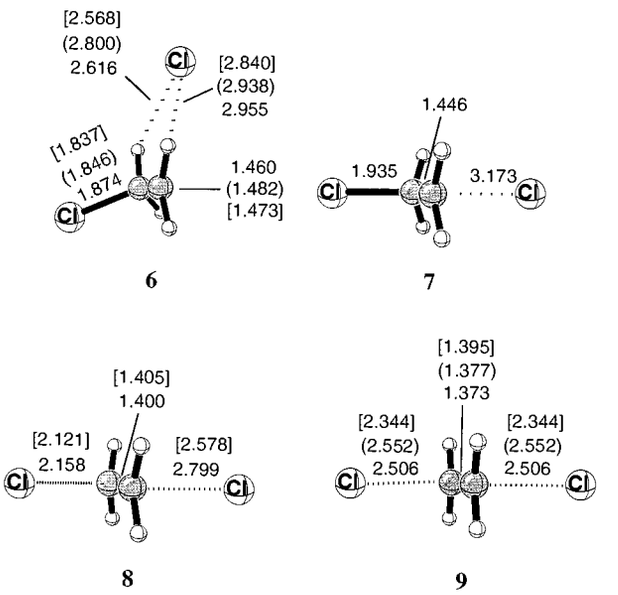

6 **7** **8** **9**

Fig. 3 Structures of ground state complexes, the transition state and the intermediate for the $S_{RN}2^c$ reaction. Structural data are given at the BHLYP/6-31+G(d,p), HF/6-31G(d) (in brackets) and MP2/6-31G(d) [in square brackets] levels of theory.

ion–dipole complex (Fig. 1), in which the chloride anion is coordinated sideways to the allyl chloride substrate (Fig. 2). The complexation energy is slightly larger now than for the S_N2 case and amounts to $\Delta E_c = -13.1$ kcal mol^{-1} at the extrapolated MP4 level of theory and to $\Delta E_c = -10.9$ kcal mol^{-1} at the BHLYP/6-31+G(d,p) + ΔZPE level. Depending on the theoretical model employed, the S_N2'-barrier for reaction through transition state **4** is 7–11 kcal mol^{-1} higher than the S_N2'-barrier. The S_N2'-barrier does, however, vary to a similar extent with the level of theory as observed for the S_N2 reaction. Thus, inclusion of a second polarization function drops the barrier by 2.7 kcal mol^{-1} at the MP2 level of theory. The extrapolated 'MP4/6-311++G(2d,2p)//MP2/6-31G(d) + ΔZPE' barrier is +19.5 kcal mol^{-1}, again close to the BHLYP/6-31+G(d,p) + ΔZPE value of +18.8 kcal mol^{-1}. The S_N2' and S_N2 reactions are also comparable in that small negative zero point energy corrections are calculated in both cases.

The ion–dipole complex **6** formed between the reactants in the $S_{RN}2^c$ reaction is closely related to complex **3** found between a chloride anion and allyl chloride in the S_N2' reaction (Fig. 3). The complexation energy is almost identical to the value obtained for the S_N2 reaction with $\Delta E_c = -9.9$ kcal mol^{-1} at the BHLYP/6-31+G(d,p) + ΔZPE level of theory (Table 1). The remaining part of the potential energy surface, however, differs dramatically from that for the S_N2 and S_N2' reactions (Fig. 1). First, the symmetric species with two identical C–Cl bond distances **9** identified as the transition state in the two closed shell cases is a shallow minimum in the $S_{RN}2^c$ case, which connects through additional transition state **8** to the ion–dipole complex **6**. The reaction path actually ends at complex **7**, in which the chloride is oriented end-on to the 2-chloroethyl radical. Complex **7** can be identified as a stationary point only at the BHLYP level of theory and is energetically slightly less favorable than complex **6**. As a second distinct difference between the open and the closed shell systems, the barrier for the substitution reaction through **8** or **9** is dramatically lower in the former case. The barrier height ΔE_a for this system is defined as the energy difference between complex **6** and transition state **8**, while the energy difference between complex **6** and intermediate **9** has been designated ΔE_b (Table 1). Basis set effects are similar to the closed shell cases and the extrapolated 'PMP4/6-311++G(2d,2p)//MP2/6-31G(d) + ΔZPE' barrier is +2.2 kcal mol^{-1}, not far from the BHLYP/6-31+G(d,p) + ΔZPE value of +1.9 kcal mol^{-1}. Inspection of Table 1 also reveals that Hartree–Fock theory is not well suited for the investigation of this system. At the UHF/6-31G(d) level, structures **7** and **8** cannot be identified as stationary points and intermediate **9** is predicted to be a transition state with a small imaginary frequency (−233 cm^{-1}) located more than 11 kcal mol^{-1} above ground state complex **6**! Optimization and frequency calculation at either UMP2/6-31G(d) or BHLYP/6-31+G(d,p), in contrast, gives all positive vibrational frequencies for **9**.

Cumulative charges for the alkyl groups in ground states **1**, **3** and **6**, transition states **2**, **4** and **8**, and for intermediate **9** have been calculated at all three levels of optimization by summation of Mulliken charges and by fitting the molecular electrostatic potential to point charges using the CHELPG scheme[11] (Table 2). Since the use of diffuse basis functions often leads to erratic charge distributions, all charges in Table 2 have been determined with the 6-31G(d) basis set. Similar values are obtained at the MP2 and the BHLYP levels of theory, while charge separation is predicted to be considerably larger at the Hartree–Fock level. Given the erratic description of the $S_{RN}2^c$ reaction at the Hartree–Fock level and the substantial deviation of the Hartree–Fock charges from the charges obtained at correlated levels of theory, results obtained at the Hartree–Fock level will not be discussed any further here. In the following we will concentrate on the BHLYP/Mulliken charges, but the same trends can also be discussed in terms of the CHELPG values and/or the MP2 level of theory.

In all three reactions depicted in Scheme 1, the alkyl groups are more positive in the transition state than in the reactant complex. The most sizable charge separation can be observed for the S_N2' reaction, in which the cumulative C_3H_5 charge is 0.21e more positive in transition state **4** than in ground state **3**. The least amount of charge separation can be found in the $S_{RN}2^c$ reaction, in which the C_2H_4 group carries only 0.11e more positive charge in transition state **8** than in ground state **6**, while the S_N2 reaction through **2** displays an intermediate behavior. The small charge separation in the $S_{RN}2^c$ reaction hints to a

Table 3 Homolytic and heterolytic bond dissociation energies (in kcal mol^{-1}) of methyl chloride, allyl chloride and 2-chloroethyl radical at the BHLYP/6-31+G(d,p) level of theory and components of the activation barrier for nucleophilic substitution with chloride according to the VBCM model

Substrate	ΔE_{hom} [a]	ΔE_{het} [a]	ΔE_{def}	B_{def}	B_{HL}	q(Alkyl) [b]	B_Q	G	f
Methyl chloride	+71.8 [c]	+ 215.7	+35.6	+ 23.1	+31.8	+0.36	+20.6	+117.2	0.30
Allyl chloride	+56.2 [d]	+ 161.3	+32.0	+ 12.4	+17.6	+0.32	+12.4	+153.7	0.21
2-Chloroethyl radical	+16.9	+ 166.4	+6.3	+5.2	—	—	—	+41.8	0.15

[a] Includes zero point energy corrections. [b] Mulliken BHLYP/6-31G*//BHLYP/6-31+G(d,p) values. [c] Exp.: +83.4 kcal mol^{-1} (ref. 12). [d] Exp.: 69.3 kcal mol^{-1} (ref. 12).

considerably larger amount of homolytic bond dissociation in the open shell systems than in either the S_N2 or the S_N2' reaction. This is also reflected in the spin density distribution obtained from the Mulliken population analysis of the BHLYP orbitals, which locates most of the spin at the former radical center (+0.69), but also some spin density at the dissociating chlorine (+0.22) as well as the former chloride anion (+0.17). In intermediate **9**, the spin density is almost uniformly distributed over the carbon and the chlorine atoms with coefficients of +0.26 and +0.27, respectively.

Discussion

If we accept the barriers calculated at either the BHLYP/6-31+G(d,p) + ΔZPE or the extrapolated PMP4/6-311++G(2d,2p)//MP2/6-31(d) + ΔZPE level as at least qualitatively correct, we are faced with the question of what the origin of the dramatically different barriers is for nucleophilic substitution in **1**, **3** and **6**. All three reactions are identity reactions and varying reaction exothermicities will therefore not be of relevance here. Since Table 1 lists intrinsic reaction barriers, we can also discard variable complexation energies for complexes **1**, **3** and **6** as the source of variations in reaction barriers. The substitution reaction involves cleavage of a carbon–chlorine bond in all three model systems, and one might therefore expect to find a correlation between the homolytic C–Cl bond dissociation energy and the S_N2 reaction barrier. The BHLYP/6-31+G(d,p) + ΔZPE bond dissociation energies listed in Table 3 can certainly explain the much lower barrier for the $S_{RN}2^c$ reaction relative to S_N2 and S_N2'. This argument is, however, not successful in rationalizing the high S_N2' barrier. As already indicated by the charge distribution in ground and transition states in Table 2, bond heterolysis will at least in part be involved in S_N2 reactions and one might hope to find a correlation between the heterolytic bond dissociation energies in reactants and reaction barriers. The BHLYP/6-31+G(d,p) heterolytic bond dissociation energies (Table 3) do indeed predict bond cleavage to be more facile in the 2-chloroethyl radical than in methyl chloride. An even lower heterolytic bond strength is, however, found in allyl chloride. We must therefore conclude that neither the homolytic nor the heterolytic C–Cl bond energies alone can be used as a guideline for the prediction of relative barriers in our three model systems.

The valence bond curve crossing model (VBCM)[5] has been applied quite successfully to nucleophilic substitution reactions in general and we will therefore attempt to rationalize the variable barrier heights in S_N2, S_N2' and $S_{RN}2^c$ reactions using this model. The VBCM model is based on the avoided crossing of the reactant and product configuration curves [Fig. 4(*a*)]. The barrier $\Delta E^‡$ is then expressed as a function of the initial electronic excitation energy G necessary to reach the product electronic configuration at the reactant structure. The crossing point of the reactant and product state curves occurs as $f \times G$, with the fractionation factor f being indicative of the slope of the curves. Finally, the transition state resonance energy B lowers the energy of the transition state below the curve crossing point. The final expression for the barrier height in identity reactions is therefore given by eqn. (1). This approximate

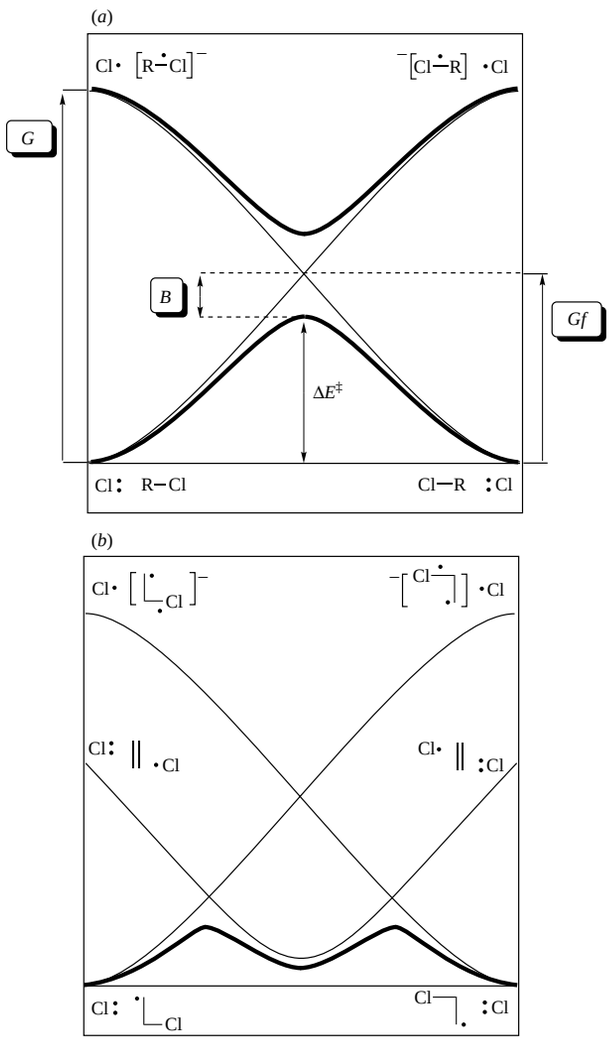

Fig. 4 State correlation diagrams for nucleophilic substitution reactions in (*a*) closed shell and (*b*) open shell substrates

$$\Delta E^‡ = Gf - B \quad (1)$$

scheme, which involves only the reactant and product Lewis configurations, can be extended to include more electronic states which might be relevant for the system under study.

Derivation of model VB wavefunctions

The first step in the VBCM analysis of our problem will be the derivation of model wavefunctions for the transition states **2**, **4** and for symmetric intermediate **9**. We begin by listing the most important configurations for each reaction in Fig. 5. For the S_N2 reaction we only consider the effective Heitler–London configurations $\Phi_{HL}(R)$ and $\Phi_{HL}(P)$ which describe the electronic configuration of reactants and products, respectively, and the triple ion configuration Φ_{TI}, in which the chlorine atoms carry a negative and the central methyl group a full positive charge. The S_N2' reaction is, in comparison, more complex.

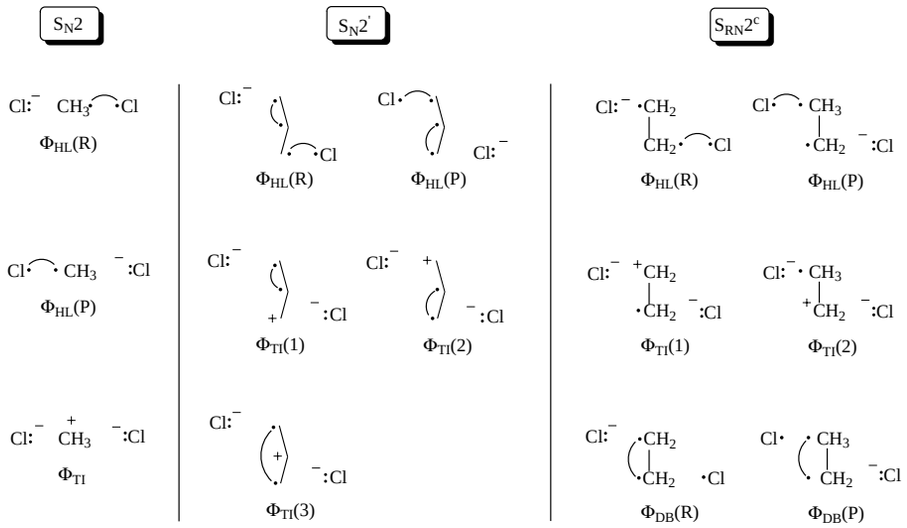

Fig. 5 The most important VB configurations for the description of the S_N2, S_N2' and $S_{RN}2^c$ reaction

In addition to the two Heitler–London configurations $\Phi_{HL}(R)$ and $\Phi_{HL}(P)$ we now have to consider three triple ion configurations $\Phi_{TI}(1)$, $\Phi_{TI}(2)$ and $\Phi_{TI}(3)$, which differ in the location of the positive charge within the C_3H_5 fragment. Description of the $S_{RN}2^c$ reaction involves two Heitler–London configurations $\Phi_{HL}(R)$ and $\Phi_{HL}(P)$ and only two triple ion configurations $\Phi_{TI}(1)$ and $\Phi_{TI}(2)$. A third type of electronic configuration can be derived from the two Heitler–London configurations by coupling the electrons situated at the two adjacent carbon atoms. Formally, this creates a double bond in the alkyl fragment and leaves the unpaired spin density on one of the chloride atoms. These two additional configurations will be designated $\Phi_{DB}(R)$ and $\Phi_{DB}(P)$.

The mixing of the three contributing S_N2 configurations into one model wavefunction starts out by generating a wavefunction Ψ_{HL} for the resonating Heitler–London state [eqn. (2)].

$$\Psi_{HL} = 2^{-\frac{1}{2}}[\Phi_{HL}(R) + \Phi_{HL}(P)] \quad (2)$$

Combination with the triple ion configuration and proper renormalization then gives the model wavefunction for the transition state of the S_N2 reaction [eqn. (3)]. The determination of the mixing coefficient a can most easily be achieved by use of the *ab initio* charge distribution. Since the CH_3 fragment carries a positive charge in Φ_{TI}, but no charge in $\Phi_{HL}(R)$ or $\Phi_{HL}(P)$, the cumulative charge for CH_3, $q(CH_3)$, is directly linked to the weight of Φ_{TI} and hence to a. Using eqn. (3), and by considering the normalization factors, this can be expressed in eqns. (4) and (5). Using the Mulliken BHLYP/6-31G(d)//BHLYP/6-31+G(d,p) charge distribution given in Table 3, a value of $a = 0.74$ is obtained.

$$\Psi_{TS} = (1 + a^2)^{-\frac{1}{2}}[\Psi_{HL} + a\Phi_{TI}] \quad (3)$$

$$q(CH_3) = a^2/(1 + a^2) \quad (4)$$

$$a = \{q(CH_3)/[1 - q(CH_3)]\}^{\frac{1}{2}} \quad (5)$$

The S_N2' model wavefunction is again constructed from the Heitler–London wavefunction Ψ_{HL} and a triple ion component, which now includes a combination of $\Phi_{TI}(R)$ and $\Phi_{TI}(P)$ as in eqn. (6). Defining the transition state wavefunction as in

$$\Psi_{TI} = 2^{-\frac{1}{2}}[\Phi_{TI}(R) + \Phi_{TI}(P)] \quad (6)$$

eqn. (7) yields an expression for the weight of the triple ion configurations which is similar to that for the S_N2 reaction. All that is different in the S_N2' cases is that a describes the weight of the combined triple ion wavefunction Ψ_{TI} and not that of individual configurations such as $\Phi_{TI}(R)$ and $\Phi_{Ti}(P)$. Evaluation of eqn. (9) using the BHLYP/6-31G(d)//BHLYP/6-31+G(d,p) value of $q(C_3H_5) = +0.32$e gives $a = 0.69$.

$$\Psi_{TS} = (1 + a^2)^{-\frac{1}{2}}[\Psi_{HL} + a\Psi_{TI}] \quad (7)$$

$$q(C_3H_5) = a^2/(1 + a^2) \quad (8)$$

$$a = \{q(C_3H_5)/[1 - q(CH_3)]\}^{\frac{1}{2}} \quad (9)$$

A more refined description is obtained upon inclusion of an additional triple ion configuration $\Phi_{TI}(3)$, in which the positive charge is located at the central carbon atom of the allyl fragment. The model wavefunction is then expressed as in eqn. (10).

$$\Psi_{TS} = (1 + a_1^2 + a_2^2)^{-\frac{1}{2}}[\Psi_{HL} + a_1\Psi_{TI} + a_2\Phi_{TI}(3)] \quad (10)$$

The equations connecting the mixing coefficients a_1 and a_2 to the charges at chlorine, the terminal CH_2-groups and the central CH-fragment can be derived as before [eqns. (11)–(13)].

$$q(CH_2) = \frac{0.5a_1^2}{1 + a_1^2 + a_2^2} \quad (11)$$

$$q(Cl) = \frac{-(0.5 + a_1^2 + a_2^2)}{1 + a_1^2 + a_2^2} \quad (12)$$

$$q(CH) = \frac{a_2^2}{1 + a_1^2 + a_2^2} \quad (13)$$

Using the BHLYP/6-31G(d) values of $q(CH_2) = +0.145$, $q(CH) = 0.033$ and $q(Cl) = -0.661$ the coefficients $a_1 = 0.64$ and $a_2 = 0.22$ are obtained. The S_N2' and S_N2 reactions are therefore rather similar in that their transition state model wavefunctions both contain a comparable and significant contribution from the triple ion configurations. The S_N2' reaction has an additional, but smaller, contribution from $\Phi_{TI}(3)$, which puts some positive charge on the central carbon atom.

Construction of the $S_{RN}2^c$ model wavefunction proceeds in a similar fashion. In addition to the resonating Heitler–London state Ψ_{HL} we now also form the resonating triple ion state Ψ_{TI} as well as the resonating double bond state Ψ_{DB} [eqns. (14)–(16)]. Combination of these three components gives the full

$$\Psi_{HL} = 2^{-\frac{1}{2}}[\Phi_{HL}(R) + \Phi_{HL}(P)] \quad (14)$$

$$\Psi_{TI} = 2^{-\frac{1}{2}}[\Phi_{TI}(1) + \Phi_{TI}(2)] \quad (15)$$

$$\Psi_{DB} = 2^{-\frac{1}{2}}[\Phi_{DB}(R) + \Phi_{DB}(P)] \quad (16)$$

model wavefunction Ψ_{TS} which now includes two mixing coefficients a_1 and a_2 [eqn. (17)]. As for the S_N2 case, values for a_1

$$\Psi_{TS} = (1 + a_1^2 + a_2^2)^{-\frac{1}{2}}[\Psi_{HL} + a_1\Psi_{TI} + a_2\Psi_{DB}] \quad (17)$$

and a_2 can be derived from *ab initio* charge densities. We can now, however, also make use of the spin density distribution (SD). Using eqn. (17), the quantitative expressions in eqns. (18)–(21) can be derived. Solving these equations for the

$$q(CH_2) = \frac{0.5a_1^2}{1 + a_1^2 + a_2^2} \quad (18)$$

$$q(Cl) = \frac{-(0.5 + a_1^2 + 0.5a_2^2)}{1 + a_1^2 + a_2^2} \quad (19)$$

$$SD(CH_2) = \frac{0.5 + 0.5a_1^2}{1 + a_1^2 + a_2^2} \quad (20)$$

$$SD(Cl) = \frac{0.5a_2^2}{1 + a_1^2 + a_2^2} \quad (21)$$

BHLYP/6-31G(d) values $q(CH_2) = +0.149$, $q(Cl) = -0.649$, $SD(CH_2) = 0.234$ and $SD(Cl) = 0.266$, the coupling coefficients $a_1 = 1.32$ and $a_2 = 1.77$ are obtained. Obviously the Heitler–London contribution is only of minor importance for the description of intermediate **9**, which appears to be dominated by the double bond and triple ion configurations Ψ_{DB} and Ψ_{TI}. This situation is reminiscent of other reactions involving the formation of intermediates such as the S_N1 or elimination reactions.[13]

Transition state resonance energy *B*

The transition state resonance energy B can be estimated by calculating the energy necessary to deform the reactants into the transition state structure, but to keep the components from interacting electronically. Subtraction of the overall reaction barrier from this deformation energy gives the resonance energy B [eqn. (22)].

$$B \approx \Delta E_{def} - \Delta E^{\ddagger} \quad (22)$$

For the S_N2 and S_N2' reactions, ΔE_{def} can be obtained by calculating the energy of the alkyl halides in their transition state structures in the absence of the chloride nucleophiles and subtracting the energy of the alkyl halides in their corresponding ground state structures. The resonance energies deduced from these energies are $B_{def}(S_N2) = +23.1$ kcal mol^{-1} and $B_{def}(S_N2') = +12.45$ kcal mol^{-1} (Table 3). For the $S_{RN}2^c$ reaction, the energy necessary to deform the chloroethyl radical in complex **6** to the structure in transition state **8** is a mere 6.3 kcal mol^{-1}. The resulting resonance energy is $B_{def}(S_{RN}2^c) = +5.2$ kcal mol^{-1}. An alternative way to estimate the resonance energy at the $S_{RN}2^c$ transition state takes intermediate **9** instead of complex **6** as the reference. The leading configuration in **9** is the double bond configuration and we can determine the deformation energy in **8** by calculating the energy of the central C_2H_4– fragment in **8** and **9**. The deformation energy for this process of $\Delta E_{def} = 5.5$ kcal mol^{-1} yields a resonance energy for transition state **8** of $B_{def}(S_{RN}2^c) = +4.7$ kcal mol^{-1}.

Following earlier work by Shaik and co-workers[14,15] on S_N2 reactions the transition state resonance energy can also be estimated using eqn. (23). This expression is based on the

$$B = \frac{1 - S_{12}}{2}\Delta E(\Psi_{TS}, \Psi^*) \quad (23)$$

assumption of two interacting states, which form resonant and anti-resonant combinations Ψ_{TS} and Ψ^*, respectively. These two combinations are separated by an energy gap of $\Delta E(\Psi_{TS},\Psi^*)$ and overlap by an integral of S_{12}. The expression for the overlap integral is given by [eqn. (24)], contains the

$$S_{12} = \frac{4s^2 + 4as + a^2}{2 + 4as + a^2} \quad (24)$$

weighing factor 'a' of the triple ion contributions as well as overlap integrals 's' between the interacting centers. Values for $\Delta E(\Psi_{TS},\Psi^*)$ and 's' can be obtained from extended Hückel (EH) calculations on the BHLYP/6-31+G(d,p) transition state geometries of **2** and **4**. The EH-parameters modified by Shaik and Reddy[15] were used for this purpose. The most simple estimate for B can be obtained by constructing the transition state wavefunction only from Heitler–London configurations, that is, setting $a = 0$ in eqn. (24). The transition state resonance energy obtained in this way is contained in Table 3 as B_{HL}. The effects of the triple ion configuration can be estimated by using the a-values derived for the S_N2 reaction ($a = 0.75$) and S_N2' reaction ($a = 0.69$). The resulting resonance energies 'B_Q' are considerably smaller than the B_{HL} values, but are, considering the approximate nature of these estimates, surprisingly close to the B_{def} values. On inspection of all the resonance energies contained in Table 3, we see that the resonance energy of the S_N2' reaction is at least 8 kcal mol^{-1} smaller than that for the S_N2 reaction and that the resonance energy for the open shell system is even smaller than that for the S_N2' reaction.

Initial gap *G*

The VB wavefunctions derived above also indicate which type of reactant electronic excitation is necessary to reach the most important electronic configuration of the transition state. For the S_N2 and S_N2' reactions, the necessary excitation is from the reactant to the product Heitler–London configuration. This can easily be calculated for the S_N2 reaction as the difference in the ionization potential of chloride $E_i(Cl^-)$ and the vertical electron affinity of methyl chloride E_{ea}(MeCl). At the BHLYP/6-31+G(d,p) level of theory, the values of $E_i(Cl^-) = 80.1$ kcal mol^{-1} and $E_{ea}(MeCl) = -37.1$ kcal mol^{-1} combine to give an initial gap of $G_{(S_N2)} = +117.2$ kcal mol^{-1}.

The calculation of $G_{(S_N2')}$ is not as straightforward, since vertical electron transfer of an electron into the ground state structure of allyl chloride locates the electron in the π* rather than the antibonding σ*(C–Cl) orbital. Use of the energetically slightly less favorable ($\Delta E = 2.8$ kcal mol^{-1}) C_s-symmetric *anti*-conformer of allyl chloride, however, solves the problem since the σ(C–Cl) and π(C–C) bonds are orthogonal now and the electron can be placed into the σ*(C–Cl) selectively. After correction for the unfavorable conformational energy of the *anti*-conformer, an initial gap of $G = 114.9$ kcal mol^{-1} is obtained. This puts the S_N2' reaction at the level of the S_N2 reaction. Comparison of $\Phi_{HT}(R)$ and $\Phi_{HT}(P)$ for the S_N2' reaction in Fig. 5, however, shows that we have come only halfway at this point as we still have to uncouple the electrons forming the allylic double bond and then recouple (as much as possible in the reactant structure) the two electrons which will form the double bond in the product. The energy required to uncouple the two electrons forming the allylic double bond can be approximated by the vertical singlet–triplet energy gap of allyl chloride, which amounts to +96.7 kcal mol^{-1} at the BHLYP/6-31+G(d,p) level of theory. This value is similar to those for ethylene (+98.5 kcal mol^{-1}) or propene (+98.6 kcal mol^{-1}) at the same theoretical

level. How much energy would be gained by recoupling the two electrons, which will form the allylic bond in the product Heitler–London state? The main difference between the π-bond just broken and the new one to be formed is the much longer C–C distance (1.487 instead of 1.325 Å) and the deformation from planarity at the methylene terminus. If the double bond in propene is deformed such that it assumes the structure of the CH_2Cl-moiety of ground state allyl chloride, the singlet–triplet gap is reduced to +40.7 kcal mol^{-1}, which is less than half of the undistorted value. Accounting for the recoupling of the allylic π-electrons, we estimated a value of $G_{(S_N2')} = +153.7$ kcal mol^{-1}. The initial gap for the S_N2' reaction therefore exceeds the gap for the S_N2 reaction by a considerable margin, which is exclusively due to the additional demand for π-electron recoupling.

The situation is completely different for the $S_{RN}2^c$ reaction, in which the initial gap corresponds to excitation from the $\Phi_{HL}(R)$ to the $\Phi_{DB}(R)$ state. In contrast to the other two cases, this does not involve electron transfer from the attacking chloride atom to the substrate but merely a recoupling of electrons within the chloroethyl radical. Formally, the chlorine–carbon single bond is broken in this process and a carbon–carbon π-bond is formed. This can be approximated as the 'vertical' C–Cl bond homolysis in radical **5**, in which the fragments retain the reactant structure. At the BHLYP/6-31+G(d,p) level of theory, a value of $G_{(S_{RN}2^c)} = +41.8$ kcal mol^{-1} is obtained. The sizable difference from the true homolytic bond dissociation energy of +16.9 kcal mol^{-1} (Table 3) results from the long C–C bond in the ethylene fragment, which does not allow for an efficient coupling of the π-bond electrons. The singlet–triplet gap in ethylene fixed in the structure of the C_2-fragment of the 2-chloroethyl radical is +57.7 kcal mol^{-1}, 40.8 kcal mol^{-1} less than in ground state ethylene.

Using the initial gaps as well as resonance energies B_{def} derived above, the fractionation factors necessary to obtain the BHLYP activation energies are 0.30, 0.21 and 0.15 for the S_N2, S_N2' and $S_{RN}2^c$ reactions, respectively. This completes the collection of components necessary for the VBCM analysis of the activation barriers for the three model systems according to eqn. (1). The high barrier for the S_N2' reaction as compared to the S_N2 reaction appears, somewhat surprisingly, not to be a consequence of the larger initial gap alone but also the lower resonance energy for the $S_{RN}2^c$ transition state. The very low barrier found for the $S_{RN}2^c$ reaction originates from the low initial gap, which is a direct consequence of the low energy double bond configuration missing in closed shell substitution reactions. Despite the crude approximations involved in the derivation of this VBCM model, it is quite interesting to note that the same rationalization can be applied to other radical-induced polar reactions such as 1,2-acyloxy-rearrangements,[3,16] or *syn*-[1,3]-elimination reactions.[17]

Acknowledgements

This work was supported by the Fonds der Chemischen Industrie. Computational resources were provided by the Zentraleinrichtung Rechenzentrum TU Berlin and Konrad-Zuse-Zentrum für Informationstechnik Berlin. I am indebted to Professor S. Shaik for numerous suggestions concerning the curve crossing model. I also thank Professor H. Schwarz for continuing support of our research.

References

1 H. Zipse, *J. Am. Chem. Soc.*, 1994, **116**, 10 773.
2 H. Zipse, *J. Am. Chem. Soc.*, 1995, **117**, 11 798.
3 H. Zipse, *J. Chem. Soc.*, *Perkin Trans. 2*, 1996, 1797.
4 (*a*) J. F. Bunnett and R. E. Zahler, *Chem. Rev.*, 1951, **49**, 273; (*b*) H. Heaney, *Chem. Rev.*, 1962, **62**, 81; (*c*) P. Müller, *Pure Appl. Chem.*, 1994, **66**, 1077. The term '$S_{RN}2$' suggested earlier[1] does not describe the regiochemistry of the reaction as precisely as '$S_{RN}2^c$'.
5 (*a*) S. S. Shaik, H. B. Schlegel and S. Wolfe, *Theoretical Aspects of Physical Organic Chemistry—The S_N2 Mechanism*, Wiley, New York, 1992; (*b*) A. Pross, *Theoretical and Physical Principles of Organic Reactivity*, Wiley, Chichester, 1995.
6 GAUSSIAN94, Revision B.3, M. J. Frisch, G. W. Trucks, H. B. Schlegel, P. M. W. Gill, B. G. Johnson, M. A. Robb, J. R. Cheeseman, T. Keith, G. A. Petersson, J. A. Montgomery, K. Raghavachari, M. A. Al-Laham, V. G. Zakrzewski, J. V. Ortiz, J. B. Foresman, C. Y. Peng, P. Y. Ayala, W. Chen, M. W. Wong, J. L. Andres, E. S. Replogle, R. Gomperts, R. L. Martin, D. J. Fox, J. S. Binkley, D. J. Defrees, J. Baker, J. P. Stewart, M. Head-Gordon, C. Gonzalez and J. A. Pople, Gaussian, Inc., Pittsburgh PA, 1995.
7 (*a*) A. D. Becke, *Phys. Rev. A*, 1988, **38**, 3098; (*b*) A. D. Becke, *J. Chem. Phys.*, 1993, **98**, 1372.
8 G. Landrum, YAeHMOP, version 1.1a, Cornell University, 1995.
9 (*a*) T. N. Truong and E. V. Stefanovich, *J. Phys. Chem.*, 1995, **99**, 14 700; (*b*) M. N. Glukhovtsev, A. Pross and L. Radom, *J. Am. Chem. Soc.*, 1995, **117**, 2024; (*c*) L. Deng, V. Branchadell and T. Ziegler, *J. Am. Chem. Soc.*, 1994, **116**, 10 645; (*d*) F. Jensen, *Chem. Phys. Lett.*, 1992, **196**, 368; (*e*) B. D. Wladkowski, K. F. Lim, W. D. Allen and J. I. Brauman, *J. Am. Chem. Soc.*, 1992, **114**, 9136; (*f*) S. C. Tucker and D. G. Truhlar, *J. Am. Chem. Soc.*, 1990, **112**, 3338; (*g*) S. R. Vande Linde and W. L. Hase, *J. Am. Chem. Soc.*, 1989, **111**, 2349; (*h*) S. C. Tucker and D. G. Truhlar, *J. Phys. Chem.*, 1989, **93**, 8138.
10 J. W. Larson and T. B. McMahon, *J. Am. Chem. Soc.*, 1985, **107**, 766.
11 C. M. Breneman and K. B. Wiberg, *J. Comput. Chem.*, 1990, **11**, 431.
12 S. G. Lias, J. E. Bartmess, J. F. Liebman, J. L. Holmes, R. D. Levin and W. G. Mallard, *Gas Phase Ion and Neutral Thermochemistry*, *J. Phys. Chem. Ref. Data*, *Suppl. 1*, 1988, 17.
13 A. Pross and S. S. Shaik, *J. Am. Chem. Soc.*, 1982, **104**, 187.
14 S. S. Shaik, E. Duzy and A. Bartuv, *J. Phys. Chem.*, 1990, **94**, 6574.
15 S. Shaik and A. C. Reddy, *J. Chem. Soc.*, *Faraday Trans.*, 1994, **90**, 1631.
16 H. Zipse, *J. Am. Chem. Soc.*, 1997, **119**, 1087.
17 H. Zipse, *J. Am. Chem. Soc.*, 1997, **119**, 2889.

Paper 7/03880A
Received 3rd *June* 1997
Accepted 22nd *August* 1997